ISSN 1063-7842, Technical Physics, 2007, Vol. 52, No. 9, pp. 1106–1116. © Pleiades Publishing, Ltd., 2007.
Original Russian Text © A.A. Koronovskii, V.I. Ponomarenko, M.D. Prokhorov, A.E. Hramov, 2007, published in Zhurnal Tekhnicheskoĭ Fiziki, 2007, Vol. 77, No. 9, pp. 6–17.

THEORETICAL AND MATHEMATICAL PHYSICS

Method of Studying the Synchronization of Self-Sustained Oscillations Using Continuous Wavelet Analysis of Univariant Data

A. A. Koronovskii[a], V. I. Ponomarenko[b], M. D. Prokhorov[b], and A. E. Hramov[a]

[a] *Saratov State University, ul. Universitetskaya 42, Saratov, 410012 Russia*
e-mail: alkor@nonlin.sgu.ru; aeh@nonlin.sgu.ru
[b] *Institute of Radio Engineering and Electronics, Russian Academy of Sciences (Saratov Branch), Saratov, 410019 Russia*
e-mail: vip@sgu.ru

Received September 5, 2006

Abstract—A new method for detecting the synchronization of a self-sustained oscillator under an external action with a linearly increasing frequency is proposed. It is based on the continuous wavelet transformation of univariant data (scalar time series). The efficiency of the method is demonstrated with a modified asymmetric van der Pol oscillator, Rössler oscillator, and experimental physiological data. In the last case, synchronization between rhythmic processes of different order in the cardiovascular and respiratory systems of the man is demonstrated using only the time series of the *R–R* intervals.

PACS numbers: 05.45.Xt, 05.45.Tp
DOI: 10.1134/S1063784207090022

INTRODUCTION

An essential component of studying a system of coupled self-oscillators is the diagnostics of synchronization modes between them. Two typical cases are usually distinguished [1–4]. The first (special) one is the synchronization of a self-sustained oscillator by an external signal generated by another self-sustained oscillator. In this case, the dynamics of the external (driving) oscillator is independent of the behavior of the driven one, while the dynamics of the driven oscillator is slaved to that of the driving one. This is referred to as synchronization between their rhythms. In the second (more general case), each oscillator exerts an influence on the other one and their interaction may either have unilateral character (which brings it closer to the first case) or be approximately symmetric. In this case, the rhythms of both oscillators are synchronized with each other. Synchronization can be characterized by ratio between the instantaneous frequencies of interacting oscillators and phase relations between their intrinsic dynamics.

In quantitative terms, synchronization between self-sustained oscillators is characterized by synchronization index [5] or synchronization degree [6, 7].

Synchronization of oscillators (including chaotic) is intensely studied today with the focus of attention increasingly shifting from radio-physical models and objects, where the basic results were obtained (see, e.g., [1–4, 6–13]), toward processes in living objects (in particular, the effect of an external drive action on an electroencephalogram [14, 15], interaction between rhythms of respiratory and cardiovascular systems [16–18], synchronization between neuron ensembles at different parts of brains of patients suffering from epilepsy [5, 19], etc.). In this sort of investigations, data are usually extracted from short time series under the conditions of excess noise. In such difficult conditions, closeness of the ratio between instantaneous frequencies to a rational number does not necessarily point to synchronism since the frequencies themselves cannot be determined to a sufficiently high accuracy. Therefore, it is the dynamics of phase relations between coupled oscillators that is most frequently studied. Under noisy conditions, the transition from an asynchronous mode to a synchronous one is rather fuzzy, and the periods of nearly constant phase difference inside the synchronous mode (it should be noted that, in the presence of noise, phase difference fluctuates in time even in a synchronous mode [3]) may be interrupted by phase jumps with a change in the phase difference by 2π. In addition, since the coupling oscillators may have a complex set of intrinsic rhythms, it is necessary to analyze synchronization and phase capture on a number of time scales inherent to the oscillators (time scale synchronization [6, 19–21]).

An illustrative example of interaction between physiological rhythms is given by functioning of the human cardiovascular system (CVS). The most significant

oscillation processes dominating the CVS dynamics are the main heart rhythm, breathing, and the slow regulation of blood pressure and heart rate with an eigenfrequency of about 0.1 Hz (the so-called Mayer wave) [22]. As a result of interaction, these rhythms are displayed in various signals: electrocardiogram (ECG), blood pressure, blood flow, and heart rhythm variability [23]. Comparatively recently, it was found that the main CVS rhythms can be synchronized [17, 24, 25]. Moreover, it was determined that the main heart rhythm can be considered as a self-sustained oscillator under the external drive action of breathing [17, 26].

In previous studies [18, 27, 28], we proposed a new method based on continuous wavelet transform to reveal synchronization of a self-sustained oscillator by an external action with linear frequency modulation and to distinguish between this situation and the admixing of external signal with the detected signal, which is taken as the sum of signals from the self-sustained oscillator and from the external source without a change in the self-oscillation frequency. Detecting the admixed external signal is important for the analysis of interaction between biological self-sustained systems of different natures to prevent erroneous conclusion about the presence of synchronization between certain biological rhythms [5, 18]. The new method proved to be effective [18, 27, 28] with the examples of a model asymmetric van der Pol oscillator and experimental physiological data on the synchronization of slow oscillations of arterial pressure under the action of breathing with a linear frequency modulation. In order to diagnose synchronization or admixing, we used the time series of external action (breathing, in the physiological experiment) and the oscillator response (*R–R* intervals derived from the ECG).

Note that, concerning the interpretation of the results of physiological experiments, of particular interest is the possibility to use univariant scalar data to diagnose synchronization between rhythms since the detection of only one scalar signal is the most accustomed practice in biological and medical applications[1] [29–32]. The aim of this study is to test the method of detecting synchronization from univariant data, i.e., from a single scalar time series (in this study, we used a series of *R–R* intervals obtained in physiological experiments). It should be noted that the necessary condition for using the proposed method is the linear or close to linear frequency modulation of the external signal.

1. EXPERIMENTAL DATA AND MODEL OSCILLATORS

Let us briefly consider the experiment that was conducted to study the interaction between the rhythms of the human CVS and respiratory system. We have tested eight healthy male volunteers aged from 20 to 34. All participants had an average level of physical activity. The ECG and breathing patterns were simultaneously recorded for each participant in a sitting position. The data were digitized at a sampling frequency of 250 Hz with 16-bit resolution and fed into a computer for the data storage and processing.

Each participant performed an experiment with breathing according to a preset rhythm with frequency f_0 varying from 0.05 to 0.30 Hz. The rhythm was set by 0.5-s-long acoustic signals, whereby the participant made a breath with each arrival of the signal. No further requirements were imposed on the way of breathing: the examinee was free to choose the convenient durations of inhalation and exhalation, as well as the breath depth. The signals were recorded for 30 min, during which the breath frequency was growing linearly.

By extracting a sequence of *R–R* intervals (representing time intervals T_i between two sequential *R* peaks) from ECG records, we obtain information on the heart rhythm variability. These series of *R–R* intervals were then the main subject of investigation.

As a simple model of interaction between the processes of breathing and slow regulation of blood pressure, we consider an asymmetric van der Pol oscillator under an external drive action with linear frequency modulation. Community between the phenomena observed in periodically excited self-sustained oscillators of physiological and physical natures was demonstrated in [18, 24, 31], where the system of heartbeat and the blood pressure regulation under the breathing action was found to exhibit qualitatively the same synchronization features as the van der Pol oscillator under a periodic external action. However, the van der Pol oscillator in self-sustained mode displays purely harmonic oscillations, while a signal detected from the CVS of a human (ECG) is considerably more complex. To test the proposed method, it was applied to analyze the synchronization of rhythms in a model oscillator with chaotic dynamics; as such, we chose the nonautonomous Rössler oscillator [33], which is often used as a basic model in the theory of chaotic synchronization [3, 4].

Thus, we used two model oscillators: first, the asymmetric van der Pol oscillator

$$\ddot{x} - (1 - x - x^2)\dot{x} + (0.24\pi)^2 x = K\sin\Phi(t) \qquad (1)$$

and, second, the Rössler oscillator

$$\begin{aligned} \dot{x} &= -y - z, \\ \dot{y} &= x + 0.15y + K\sin\Phi(t), \\ \dot{z} &= 0.2 + z(x - 10) \end{aligned} \qquad (2)$$

under an external drive action with linear frequency modulation. In Eqs. (1) and (2), K is the amplitude of

[1] In particular, in application to CVS studies, this means the possibility to analyze synchronization using the data of halter belts applied for long-term cardiovascular monitoring.

the external signal and phase

$$\Phi(t) = 2\pi[(\gamma + \beta t/T)]t \quad (3)$$

specifies the linear time function of external frequency ω_d,

$$\omega_d(t) = \frac{d\Phi(t)}{dt} = 2\pi(\gamma + 2\beta t/T), \quad (4)$$

where t is current time; parameters $\gamma = 0.03$, $\beta = 0.17$, and $T = 1800$ (maximal time of calculation) for the van der Pol oscillator (1); and $\gamma = 0.01$, $\beta = 0.25$, and $T = 3200$ for the Rössler oscillator (2). The parameters were chosen in accordance with the data of [18].

Equations (1) and (2) for the asymmetric van der Pol oscillator and the Rössler oscillator were solved numerically using the Runge–Kutta fourth order method with time step $\Delta t = 0.010$ and 0.004, respectively.

To analyze and compare the cases of synchronization by an external signal and admixing of the external signal with the detected oscillations, we analyze the sum signal

$$x_\Sigma(t) = x(t) + R\sin\Phi(t), \quad (5)$$

where $x(t)$ is the solution to Eq. (1) for the autonomous asymmetric van der Pol oscillator or to Eq. (2) for the Rössler oscillator, R is the amplitude of the admixing signal, and phase $\Phi(t)$ of the additive signal is given by (3).

2. METHOD FOR DETECTING THE SYNCHRONIZATION OF SELF-SUSTAINED OSCILLATIONS USING WAVELET ANALYSIS OF UNIVARIANT (SCALAR) TIME SERIES

2.1. Phase Dynamics of a Constant Scale Corresponding to the Frequency of Self-Sustained Oscillations

The main idea of the method proposed for the detection of synchronization from univariant data (scalar time series) consists in the analysis of the time dependences of quantity $\Delta\varphi_0(t)$, which is the variation of phase $\varphi_{s0}(t)$ of the first harmonic (with frequency f_0) of self-sustained oscillations between time moments t and t–τ:

$$\Delta\varphi_0(t) = \varphi_{s0}(t) - \varphi_{s0}(t - \tau), \quad (6)$$

where time shift parameter τ can be varied in a wide range. Phase difference $\Delta\varphi_0(t)$ will be understood as the difference between the phases of signal generated by the nonautonomous oscillator at different time moments in response to the external action.

Phase $\varphi_{s0}(t)$ of the first harmonic of the external signal is introduced using the approach based on the wavelet transform of signals with a complex basis [6, 7, 20, 21, 34]. The continuous wavelet transform [35, 36] of time series $x(t)$ is given by the convolution

$$W(s, t_0) = \int_{-\infty}^{+\infty} x(t)\psi^*_{s, t_0}(t)dt, \quad (7)$$

where $\psi_{s, t_0}(t)$ is the wavelet function obtained from the generating wavelet $\psi_0(t)$,

$$\psi_{s, t_0}(t) = \frac{1}{\sqrt{s}}\psi_0\left(\frac{t - t_0}{s}\right). \quad (8)$$

Time scale s determines the width of wavelet $\psi_{s, t_0}(t)$ and t_0 is the time shift of the wavelet function along the time axis (asterisk denotes complex conjugation). It should be noted that the concept of time scale s in wavelet analysis plays the role similar to that of frequency f (or period $T = 1/f$) in Fourier transformation.

Wavelet spectrum

$$W(s, t_0) = |W(s, t_0)|\exp[j\varphi_s(t_0)] \quad (9)$$

characterizes the behavior of the system at every time scale s at an arbitrary time moment t_0. Absolute value $|W(s, t_0)|$ characterizes the presence and intensity of the corresponding time scale s at time t_0. As the generating wavelet in (8), we take the complex Morlet wavelet [37]

$$\psi_0(\eta) = (1/\sqrt[4]{\pi})\exp[j\sigma\eta]\exp[-\eta^2/2].$$

Here, parameter σ determines the properties of wavelet transform with the generating Morlet wavelet [36]. Let us use the parameter $\sigma = 2\pi$, which provides a simple relation between the Fourier frequencies and scales $f = 1/s$ [36].

Introducing the phase in the described manner—via a continuous wavelet transform—makes it possible to effectively analyze systems with an uncertainly determined phase, when no continuous phase can be correctly defined (including the case of a chaotic signal [6, 20, 21]).

A necessary condition to apply the proposed method for the analysis of phase difference (6) is that the frequency of the external signal should grow with time and pass sequentially through the synchronization ranges (1 : 1), (1 : 2), …, (1 : n), …, (m : n), …, ($n \in \mathbb{Z}$), etc. Indeed, in the time intervals corresponding to asynchronous dynamics of the system (far from synchronization (m : n), so that the external signal has almost no influence on the dynamics of the basic frequencies in the spectrum of self-sustained oscillations), phase difference (6) must remain constant. In the time intervals corresponding to asynchronous dynamics of oscillations, the signal phase changes linearly with time $\varphi_{s1}(t) = 2\pi f_0 t + \bar{\varphi}$, where f_0 is the self-sustained frequency of the oscillator and $\bar{\varphi}$ is the initial phase. Then, according to definition (6), phase difference in the case of periodic self-sustained oscillations $\Delta\varphi_0(t) = 2\pi f_0\tau$, i.e., has a constant value.

However, in the vicinity of time moments t_{ns}, when the external frequency is close to the eigenfrequency of the oscillator (within the synchronization ranges), phase difference $\Delta\varphi_0(t)$ (6) must behave principally differently.

Inside the synchronization tongue, phase difference $\Delta\tilde{\phi}(t) = \varphi_{s1}(t) - \varphi_{ext}(t)$ between phase $\varphi_{s1}(t)$ of the oscillator's response and phase $\varphi_{ext}(t)$ of the external signal can be described by the Adler equation [38], which for the asymmetric van der Pol oscillator under external drive action with a variable frequency has the form [18]

$$\frac{d(\Delta\tilde{\varphi}(t))}{dt} + \kappa\sin\Delta\tilde{\phi}(t) - (2\pi f_0 - \omega_d(t)) = 0. \quad (10)$$

It follows from the Adler equation that phase difference $\Delta\tilde{\phi}(t)$ in a synchronization region of the (1 : 1) type must change by π. Since the phases of the oscillator's response at time moments t and $t + \tau$ are equal to $\varphi(t) = \int_0^t \omega_d(t)dt$ and $\varphi(t) = \int_0^{t-\tau} \omega_d(t)dt$ and in view of a finite width of the wavelet function in the Fourier space [36] and formula (4), the values of $\Delta\varphi_0(t)$ (6) can be written in the form

$$\Delta\varphi_0(t) = \int_{t-\tau}^{t} \omega_d(t)dt = 2\pi\left(\gamma + \frac{2\beta t}{T}\right)\tau - 2\pi\frac{\beta}{T}\tau^2 + \gamma, \quad (11)$$

where $\gamma = \Delta\tilde{\phi}(t) - \Delta\tilde{\phi}(t-\tau) \approx$ const is a constant (in the first approximation) correction to the phase difference due to synchronization under the external signal. The second and third terms in (11) are constants $C = \gamma - 2\pi\beta/T\tau^2$ = const. Then, with allowance for (4), the phase difference appears in the form

$$\Delta\varphi_0(t) = \omega_d(t)\tau + C. \quad (12)$$

The expression above suggests that, as the external frequency passes through the synchronization region, function $\Delta\varphi(t)$ changes by the value

$$\Delta\varphi_s \approx (\omega_d(t_2) - \omega_d(t_1))\tau = \Delta\omega\tau, \quad (13)$$

where frequencies $\omega_d(t_1)$ and $\omega_d(t_2)$ correspond to the left (low-frequency) and right (high-frequency) boundaries of the synchronization (Arnold) tongue and $\Delta\omega$ is the synchronization range width.

The above considerations refer to the case of the 1 : 1 synchronization, when external frequency f_d and eigenfrequency f_0 of the oscillator relate as $f_d/f_0 = 1$. However, the described approach can be generalized to a more complex case of $n : m$ synchronization. In this case, function $\Delta\varphi(t)$ will be replaced by

$$\Delta\varphi_s = \frac{m}{n}\Delta\omega\tau. \quad (14)$$

Thus, analyzing phase difference in the form (6), one should distinctly distinguish between synchronization modes and modes of asynchronous dynamics. In particular, phase difference $\Delta\varphi_0(t)$ is constant in an asynchronous mode and changes by a certain value $\Delta\varphi_s$ specified by (14) as the external frequency passes the Arnold tongue. This behavior of phase difference (6) provides a reliable criterion for discrimination between the different modes of the nonautonomous oscillator.

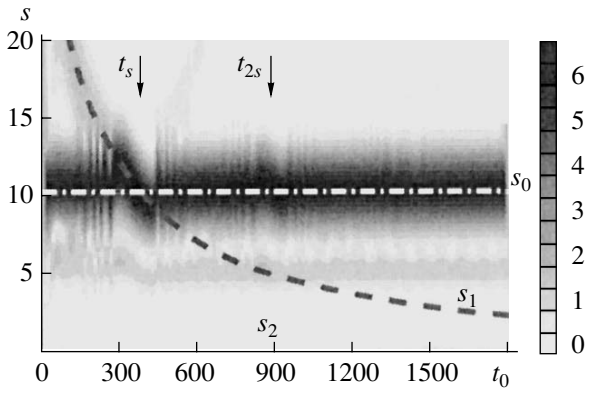

Fig. 1. Wavelet spectrum $|W(x, t_0)|$ of signal generated by the asymmetric van der Pol oscillator (1) at $\alpha = 1.0$ under external drive action with linear frequency modulation $\omega_d(t)$ (4). The abscissa is the time, and the ordinate is the time scales. The grey color intensity is proportional to wavelet coefficients $|W(s, t_0)|$ in accordance with the gradient palette on the right. Dashed curve s_1 corresponds to the first harmonic of external signal $\omega_d/2\pi$; and dash-and-dot curve s_0, to frequency f_0 of the self-sustained oscillations.

Let us now consider the results given by the method in application to the asymmetric van der Pol oscillator (1) taken as the model oscillator. To introduce the phase of the first harmonic with frequency f_0, we use the continuous wavelet transform of the oscillator's response to the external drive action. Phase difference is constructed along the constant time scale s_0 corresponding to Fourier frequency f_0 in the spectrum of an autonomous van der Pol oscillator. The wavelet transform is constructed using the Morlet generating wavelet and parameter $\sigma = 2\pi$.

Figure 1 shows the amplitude wavelet spectrum in the coordinates of time shift t_0 and wavelet transform scale s, plotted during time $T = 1800$. Dashed line s_1 marks the dynamics of scale $s_1(t)$ corresponding to the first harmonic with frequency $\omega_d(t)$ (4) of the external signal. The analysis of the wavelet spectrum bears evidence of the classical entrapping of the oscillation frequency by the external signal; this is confirmed by the bends appearing at time moments t_s and t_{2s} (marked by arrows), when the external frequency is close to the frequency $\omega_d(t_s) \approx 2\pi f_0$ of the autonomous oscillator or its second harmonic $\omega_d(t_{2s}) \approx 4\pi f_0$ (marked at the wavelet spectrum). This bend represents the effect of pulling of the oscillation frequency by the external signal and the following return of this frequency and its harmonics to the self-sustained frequency at a large detuning ω_d–$2\pi f_0$.

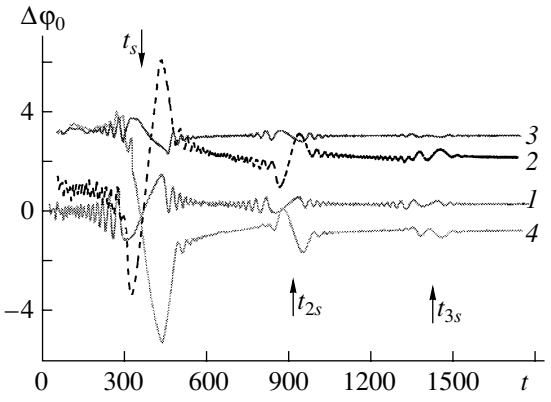

Fig. 2. Dynamics of phase difference $\Delta\varphi_0(t)$ (6) at the time scale s_0 corresponding to the first harmonic $f_0 = 0.0973$ of self-sustained oscillations of the asymmetric van der Pol oscillator (1).

Figure 2 shows the dynamics of phase difference $\Delta\varphi_0(t)$ (6) at the self-sustained frequency of the oscillator (corresponding scale s_0 is shown dashed in Fig. 1) for the time shift $\tau = 25.5$ (curve *1*). It is seen that dependence $\Delta\varphi_0(t)$ includes almost constant portions, where the external frequency is far from eigenfrequency f_0 of the oscillator and its harmonics nf_0 (the modes of asynchronous dynamics). There are also the portions of monotonic variation of phase, which are observed at time moments t_{ns}, when the external frequency $\omega_d(t_{ns}) \approx 2\pi nf_0$ (synchronization modes).

It should be noted that this method has a number of advantages over the previously proposed technique, in which the phase difference was detected on a variable scale corresponding to the varying external frequency [18, 28]. First, the regions of monotonic variation of phase (which correspond to synchronization modes) are readily detected against the background of a constant phase difference in the asynchronous mode and, second, this method offers an appreciably higher accuracy since the dynamics of the phase difference is considered at the time scales that have high amplitudes in the wavelet spectrum. In particular, time dependence of phase difference $\Delta\varphi_0(t)$ contains a well-defined region of the 1 : 3 synchronization at the third harmonic $3f_0$ of the fundamental frequency (marked as time moment t_{3s} in Fig. 2). Note also that this method is much easier to implement than the method [18, 28] based on the analysis of phase difference at a variable time scale.

Apparently, the presence of synchronization (especially for high orders ($m : n$) or in the case of a distorted signal, for example, in noisy conditions) is more readily detected if the swing of the monotonic variation of $\Delta\varphi_0$ is enhanced when passing through the $m : n$ synchronization region. As follows from (13), this can be achieved by increasing time shift parameter τ in (6). An increase in τ evidently leads to the growth of phase difference $\Delta\varphi_0$ within the synchronization region, thus, increasing the possibility to reveal the synchronous mode while scanning external frequency $\omega_d(t)$. These considerations are illustrated in Fig. 2 (curve *2*, for $\tau = 85$). In this case, the phase difference grows by a factor of ~4 compared with curve *1* ($\tau = 25.5$), as might be expected from formula (13).

Note that choosing parameter τ negative can provide a monotonic decrease in phase difference $\Delta\varphi_0(t)$ in the synchronization region. Such a decrease is particularly convenient for the detection of synchronization from real data. An example is given in Fig. 2 by curves *3* and *4* plotted for time shifts $\tau = -10.8$ and -55.5, respectively. It is clearly seen that the dynamics of the phase is qualitatively similar to that described above but the run of the curves at the synchronization regions is changed for the inverse one. It is also seen that, as before, the larger the absolute value of τ, the larger the swing of phase difference $\Delta\varphi_0(t)$ at the synchronization regions (compare the amplitudes of changes in the phase difference in curves *3* and *4*).

2.2. Effect of Noise and Uncertainty in Determining the Basic Time Scale by the Example of van der Pol Oscillator

Note that time series extracted from real experimental data (especially, obtained from living objects) are characterized by a certain noise level distorting the useful signal. Moreover, some parameters (e.g., fundamental frequency) of the autonomous dynamics of biological systems cannot be determined with a required accuracy. In particular, in application to the analysis of the human CVS and respiratory system, it is practically impossible to study the autonomous CVS dynamics since both systems permanently interact with each other, even in an arbitrary breathing mode. Therefore, it is by no means possible to determine precisely the self-sustained frequency of basic CVS rhythms of a patient. In this context, an important question arises on the extent to which the proposed approach can be relied on if the time series contain additive noise or the frequencies of the basic rhythms in a studied system are determined with a low accuracy.

As above, we will examine this problem using the model of asymmetric van der Pol oscillator (1) under the external drive action with linear frequency modulation (4). To allow for the effect of noise on the detection of synchronization, let the time signal be taken in the form

$$x_n(t) = x(t) + D\zeta(t), \tag{15}$$

where $x(t)$ is the solution to the autonomous equation of the asymmetrical van der Pol oscillator (1), $\zeta(t)$ is an additive noise with zero average and uniform distribution within the [–0.5, 0.5] interval, and D is the noise intensity. Noise $\zeta(t)$ is modeled by standard random series, as described in [39].

The possibility of detecting a synchronization mode was studied at different levels of the additive noise obscuring the synchronization effect. Figure 3a shows typical time series (15) in the synchronization mode for different intensities of the additive noise. It is seen that the noise highly distorts the signal but not the wavelet spectrum. A convincing example is the amplitude wavelet spectrum (Fig. 3b) obtained at $\sigma = 2\pi$ for an additive noise with intensity $D = 10$. Comparison between Fig. 3b and Fig. 1 for a time series in the absence of noise suggests that, despite of the distortions, the wavelet spectrum preserves the main features of the oscillation dynamics; specifically, time scale s_0 corresponding to the first harmonic of frequency f_0 of the van der Pol oscillator is clearly discerned (dot-and-dash line in Fig. 3b) and the effect of frequency pulling at the region of (1 : 1) synchronization is observed (shown by the arrow in Fig. 3b). Hence, it follows that applying the wavelet transform to determine the phases of harmonics in a studied signal makes it possible to extract synchronization modes from a noisy time series.

Figure 3c shows phase difference $\Delta\varphi_0(t)$ (6) calculated using the value of time shift $\tau = 25.5$ and the generating wavelet with parameter $\sigma = 2\pi$ for different noise intensities D. It is clearly seen that the time dependences of the phase difference become increasingly more indented; however, for all the noise intensities, a time interval can be found during which the phase difference varies almost monotonically and is numerically equal to the phase difference calculated from the data in the absence of additive noise (see the magnified fragment of the time interval corresponding to the (1 : 1) synchronization mode in Fig. 3d). Thus, the presence of additive noise with a fairly high intensity does not preclude the detection of synchronization using univariant time data in terms of the proposed approach. At a very high noise intensity $D = 10$, the presence of synchronous dynamics is less distinct (Figs. 3c, 3d), but it should be noted that the noise amplitude is nearly twice the amplitude of the signal in this case. Note also that, at such a high noise amplitude (Fig. 3c, the curve corresponding to $D = 10$), the phase difference slowly grows during the asynchronous oscillation modes. This effect is due to the presence of noise, which alters the dynamics of instantaneous phase $\varphi_{s0}(t)$ of the first harmonic as compared to the case $D = 0$. At large noise intensities $D > 5$, high-order synchronization modes are indistinguishable because of the phase fluctuations, which become comparable with the monotonic variation of the phase. One possibility to improve the situation is to analyze phase difference (6) for larger values of parameter τ, thus, raising the resolution of the method. As was shown in Section 2.1, an increase in τ enlarges the swing of the phase difference within the synchronization range, while the noise-induced fluctuations remain constant. Therefore, the higher synchronization modes can be detected.

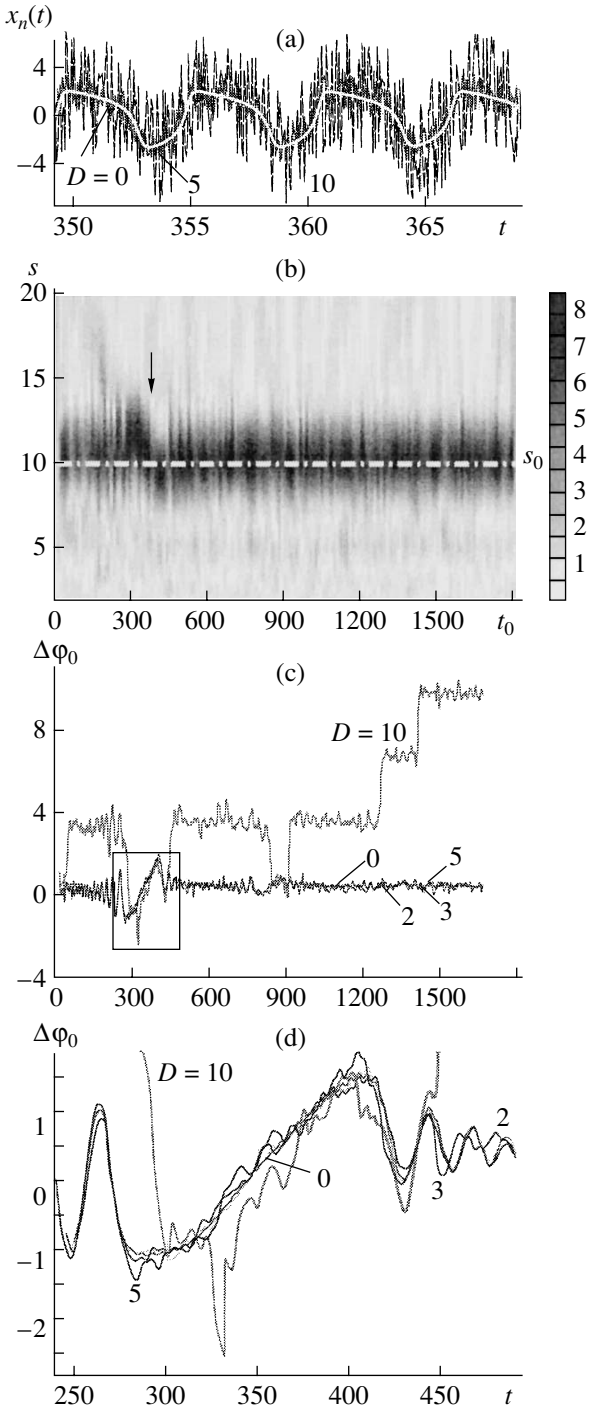

Fig. 3. (a) Typical time series of sum signal $x_n(t)$ from the van der Pol oscillator in the (1 : 1) synchronization mode for different noise intensities D (15); (b) wavelet spectrum $|W(s, t_0)|$ of sum signal $x_n(t)$ for $D = 10$, $\alpha = 1.0$, $K = 0.2$, and $\sigma = 2\pi$; (c) time dependences of phase difference $\Delta\varphi_0(t)$ (6) for different noise intensities (indicated by figures near the corresponding curves).

Let us now consider the detection of synchronization in case of a fuzzy specification of time scale s along which the phase difference dynamics is calculated. As was discussed above, such a problem arises when it is

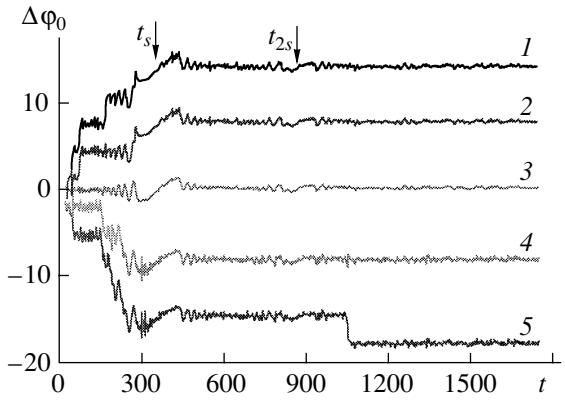

Fig. 4. Phase difference $\Delta\varphi_0(t)$ at a time scale $s_1 = s_0 + \Delta s$ approximately matching the scale $s_0 = 1/f_0 = 10.28$ of the autonomous van der Pol oscillator, s_1 = (*1*) 11.46 > s_0, (*2*) 11.24 > s_0, (*3*) 10.28 = 2s_0, (*4*) 8.55 < s_0, and (*5*) 8.52 < s_0.

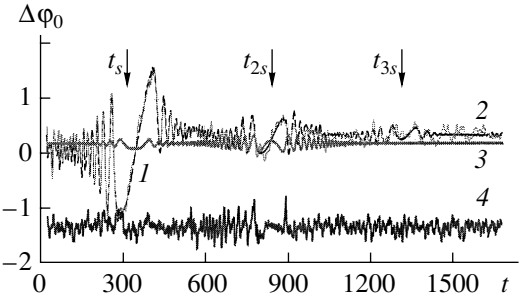

Fig. 5. Time dependences of phase difference $\Delta\varphi_0(t)$ for the van der Pol oscillator in the case of (*1*, *2*) synchronization by an external signal with amplitude $K = 0.2$ and (*3*, *4*) admixing of the external signal with amplitude $R = 0.2$. The parameter of the time shift is $\tau = 25.5$, the noise intensity $D = 0$ (*1*, *3*) and $D = 3$ (*2*, *4*).

impossible for some reason to determine exactly the eigenfrequency of self-sustained oscillations. Let us analyze the behavior of phase difference $\Delta\varphi_0(t)$ specified at the time scale $s_1 = s_0 + \Delta s$, where Δs is the detuning of time scale s from basic scale s_0 of the self-sustained oscillations. The dynamics of phase difference calculated for different time scales is shown in Fig. 4. The calculation is carried out for sum signal (15) with the noise intensity $D = 3$ and the time shift $\tau = 25.5$. At small detunings $\Delta s < 0.5$–1.0, the dynamics of the phase difference is generally the same as in the case of exact match to basic time scale s_0. At high Δs, as is evident from Fig. 4, the phase difference grows with time. Along with this growth, at the regions of synchronization (marked by arrows), a monotonic variation of phase difference $\Delta\varphi_0(t)$ is distinctly displayed at the frequency close to the fundamental frequency of the self-sustained oscillator. Therefore, to detect synchronization with the method proposed, it suffices to know an approximate value of basic time scale s_0 (of frequency f_0) in the self-sustained dynamics of the oscillator.

On the basis of the results obtained from the consideration of the model system, one can infer that the proposed method for detecting synchronization is highly immune to noises and uncertain data. This robustness is largely due to the properties of continuous wavelet transform.

2.3. Comparison between Synchronization and Admixing of External Signal by the Example of van der Pol Oscillator

Now, we briefly concern the problem of recognition of the situation when the external signal admixes with a time series under study. This problem was considered in detail in [18] in application to the processing of physiological data. As was discussed in the introduction, the systems that set the main heart rhythm and the rhythm of slow regulation of the blood pressure can be considered as self-sustained oscillators under external drive action of breathing [17, 26]. However, at breathing frequencies close to 0.1 Hz, i.e., to the eigenfrequency of the blood regulation rhythm, it becomes difficult to discriminate between synchronization of these two processes and the influence of the respiratory component present in the heart rhythm variability (*R*–*R* intervals), which is used to analyze the slow oscillations of the blood pressure. The dynamics of human CVS is a result of an intricate interaction between various physiological processes [40], and their contributions to the heart rhythm variability can hardly be separated if their frequencies are close. For this reason, it seems important to search for a method that will make it possible to separate the synchronization of oscillations by an external action from the admixing of the external signal with the oscillator's signal without interaction between them. It was demonstrated in [18] that a principally important point in solving this problem is the use of an external action with a variable frequency. Let us briefly consider how the method for detecting synchronization from univariant data can be applied to detect an admixing external signal in the absence of synchronization. The admixing signal is taken in the form of sum signal x_Σ (5).

Figure 5 shows the time dependences of phase difference $\Delta\varphi_0(t)$ that are plotted for the cases of synchronization and admixing of the external signal in the absence and presence of additive noise ($D = 0$ and 3, respectively). Comparing the cases of synchronization (curves *1* and *2* for $D = 0$ and 3, respectively) and admixing (curves *3* and *4* for $D = 0$ and 3, respectively) suggests that the phase difference in the second case is almost constant in time and, hence, is independent of the frequency of the external signal, which is additively summed with the oscillator signal (5). In the case of admixing, $\Delta\varphi_0(t) \approx \Delta\varphi_{1,2} = \text{const}$ at any time moment independently of the offset of the external frequency from the frequency of self-sustained oscillations. In the case of synchronization, dependence $\Delta\varphi_0(t)$ displays the behavior that is already known, i.e., monotonically varies within the synchronization range.

In terms of this approach, the admixing of the external signal with the output signal without synchronization is especially easy to detect as compared to the earlier proposed method [18] based on the analysis of the phase difference between the external signal and the response of the nonautonomous system at a variable frequency of the external action. In this case, the shape of dependence $\Delta\varphi_0(t)$ had to be analyzed at the time moments when the external frequencies coincide with the frequencies of self-sustained oscillations (for more details, see [18]); such an analysis seems difficult to perform given the time series of the oscillations in the presence of high-level noises.

Thus, the proposed method for detecting synchronization is based on the measurement of phase difference (6) at the eigenfrequency of the oscillator subjected to an external drive action with a linear frequency modulation. Instantaneous phase of a harmonic to be analyzed is introduced by means of continuous wavelet analysis with a complex Morlet wavelet. The main advantage of the method is the possibility to analyze the synchronization of oscillations using a single scalar time series (univariant data) of the oscillations in response to the external drive action. The proposed method proves to be stable to the presence of parasitic noises in the time series and can be applied without knowing exactly the characteristics related to the autonomous dynamics of the oscillator. Both conditions are typical of physiological data; therefore, the method can be effective for the analysis of self-sustained oscillations of biological nature. Moreover, the proposed method provides an opportunity to distinguish between the situations when the external signal synchronizes self-sustained oscillations and when it admixes with the detected signal without interacting with it (the detected signal is meant as a sum of signals at a fixed frequency of the self-sustained oscillations).

Analysis of the applicability conditions shows that the proposed method can be used provided that the frequency of the external drive action is modulated by a certain law. The possibility to fulfill this condition depends on a particular system under study and the layout used in the experiment.

3. ANALYSIS OF SYNCHRONIZATION OF CHAOTIC SELF-SUSTAINED OSCILLATIONS BASED ON UNIVARIANT DATA FOR THE RÖSSLER OSCILLATOR

In the previous section, the new method proposed for detecting synchronization from univariant (scalar) data was described in detail by the example of the asymmetric van der Pol oscillator (1). Now, we analyze the applicability of the method in the case of chaotic self-sustained oscillations under an external drive action. As a model, we use the Rössler oscillator in the chaotic oscillation mode under an external action with a variable frequency. The Rössler oscillator (2) in the autonomous mode displays chaotic oscillations with a well-defined fundamental frequency $f_0 = 0.163$, a high noise pedestal, and the second $2f_0$ and third harmonics $3f_0$ standing out against this background.

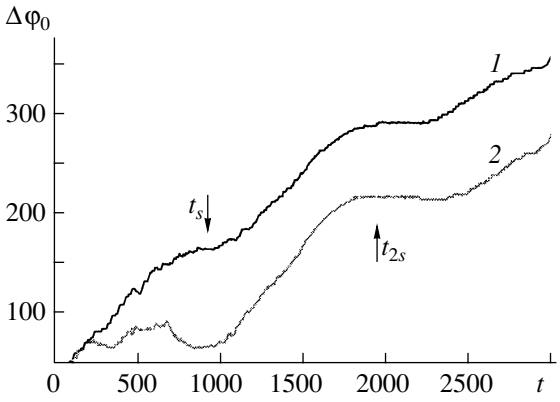

Fig. 6. Dynamics of phase difference $\Delta\varphi_0(t)$ (6) at time scale s_0 corresponding to the first harmonic $f_0 = 0.1631$ of self-sustained chaotic oscillations of the Rössler oscillator (2); instantaneous phases are calculated with the use of the Morlet wavelet with $\sigma = 2\pi$, time shift $\tau = 12.2$, and the amplitudes of the external action $K =$ (*1*) 1.5 and (*2*) 3.0.

Consider two cases of the external action with different amplitudes $K = 1.5$ and 3.0 and variable frequency (4). As above, the phase of the first harmonic with frequency f_0 is introduced with the help of the continuous wavelet transform of oscillations in response to the external action. The phase difference is constructed along the constant time scale $s_0 = 6.135$ corresponding to Fourier frequency $f_0 = 0.163$ in the spectrum of the autonomous Rössler oscillator. The wavelet transform is generated using the Morlet basis function and parameter $\sigma = 2\pi$.

The resulting dynamics of phase difference $\Delta\varphi_0(t)$ (6) is shown in Fig. 6. The arrows mark the time moments when the external frequency is close to the frequency of self-sustained oscillations or its second harmonic (entrapping of the basic frequency in the nonautonomous mode, the synchronization mode). It is clearly seen that, in the asynchronous modes of the chaotic signal (the external frequency is far from the frequency of self-sustained oscillations), phase difference $\Delta\varphi_0(t)$ rapidly drifts. In the synchronization region, the phase difference stabilizes and monotonically varies by a value close to that specified by (14). This behavior of the phase difference is due to the fluctuations of phase of the chaotic signal, which are responsible for the change in phase difference $\Delta\varphi_0(t)$ in the region of asynchronous behavior.

Thus, when applied to the detection of synchronization of chaotic self-sustained oscillations, our method predicts that phase difference $\Delta\varphi_0(t)$ rapidly varies in the asynchronous modes and meets conditions (13) or (14) in the synchronization modes. Note that the variations of the phase difference in the asynchronous region

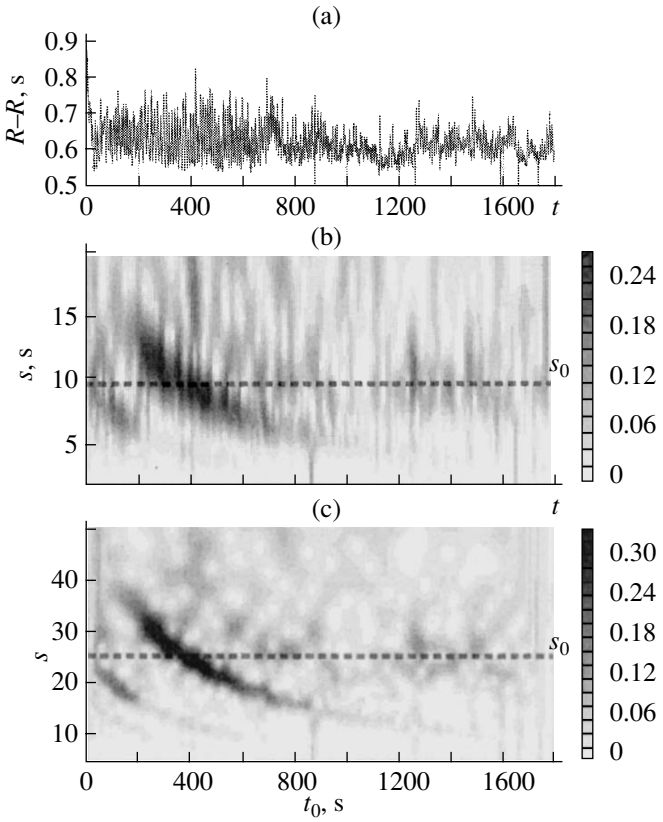

Fig. 7. (a) A time series of the *R–R* intervals typical of the case of breathing with a linearly increasing frequency and the corresponding wavelet spectra generated using the Morlet wavelets with parameter σ = (b) 2π and (c) 16. Dashed line marks the time scale along which phase difference $\Delta\varphi_0(t)$ is calculated; the scale corresponds to the Mayer wave frequency f_0 = 0.1 Hz.

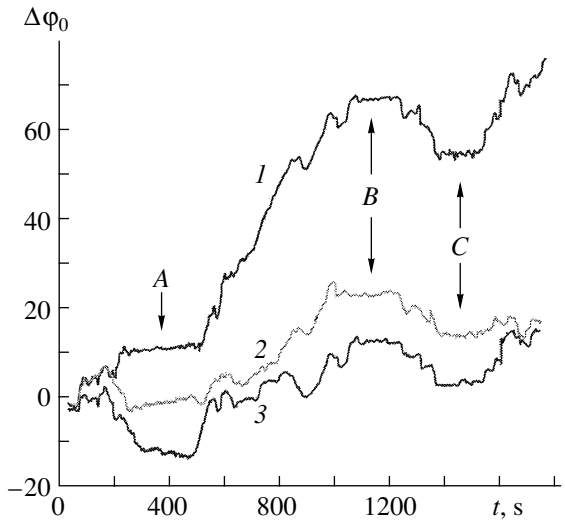

Fig. 8. Dynamics of phase difference $\Delta\varphi_0(t)$ at time scale s_0 corresponding to the frequency f_0 = 0.1 Hz of the Mayer wave for breathing with a linearly increasing frequency: calculation from a series of the *R–R* intervals using the Morlet generating wavelet and time shift τ = (*1*) 10 (with σ = 2π), (*2*) 16.42 (σ = 16), and (*3*) –5.25 s (σ = 2π).

may have different character (cf. curves *1* and *2* in Fig. 6 for different amplitudes of the external action).

4. SYNCHRONIZATION BETWEEN THE RHYTHMS OF THE HUMAN CARDIOVASCULAR SYSTEM AND RESPIRATORY SYSTEM USING UNIVARIANT DATA FOR THE HEART RHYTHM VARIABILITY

Let us now turn to the analysis of interaction between the rhythms of the human CVS and respiratory system using univariant data on the heart rhythm variability, which were the series of the *R–R* intervals extracted from the ECG of the voluntary participants of the experiment. The experimental technique was described in Section 1.

Figure 7a shows a typical time series of the *R–R* intervals extracted from the ECG of participants whose breathing frequency was linearly modulated. The series of the *R–R* intervals is nonequidistant, i.e., time interval T_i between two neighboring samples in the series is not the same. A special technique was invented to perform a continuous wavelet transform of a time series with nonequidistant time samples. Figures 7b and 7c show wavelet spectra $|W(s, t_0)|_0$ constructed using the Morlet wavelets with parameters $\sigma = 2\pi$ and 16, respectively, for a series of *R–R* intervals obtained at linear modulation of the breathing frequency. A wavelet transform with a larger σ provides for a higher frequency resolution [36], which is required to extract more accurately the dynamics of the time scales corresponding to the 0.1 Hz rhythm and the external signal of breathing with a variable frequency. It should be noted that the time scales of a wavelet transform with $\sigma = 2\pi$ coincide with the Fourier transform periods and are measured in seconds. In the wavelet transform with $\sigma = 2\pi$, the time scales are renormalized according to the formula [36]

$$s = \frac{\sigma + \sqrt{\sigma^2 + 2}}{4\pi f}, \qquad (16)$$

where s stands for the time scales of the wavelet transform and f takes the values of the Fourier frequencies (this circumstance explains the difference in the ordinate axes in Figs. 7b and 7c).

As seen from Figs. 7b and 7c, wavelet spectra $|W(s, t_0)|$ constructed at different values of σ from the time series of *R–R* intervals under a linear modulation of the breathing frequency display an intense signal corresponding to the breathing frequency. The intensity of the rhythm with the frequency f_0 = 0.1 Hz, or the time scale (period) T = 10 s (Mayer wave), is small compared to the amplitude of the external signal and appears only faintly in Figs. 7b and 7c.

Following the proposed algorithm (6), we analyze phase difference $\Delta\varphi_0(t) = \varphi_{s0}(t) - \varphi_{s0}(t - \tau)$ at time scale s_0 (shown dashed in Figs. 7b, 7c) corresponding to the

frequency of the Mayer wave and specified by relationship (16).

Figure 8 presents time dependences $\Delta\varphi_0(t)$ of phase difference between the harmonics of the Mayer-wave frequency as obtained from the series of *R–R* intervals for difference values of time shift τ.

The plot demonstrates the existence of such time intervals (and, hence, the frequency ranges since the external frequency is a linear time function) where the behavior of the phase difference is, on average, close to linear (such regions are marked by arrows in Fig. 8). This circumstance indicates that different-order synchronization modes are set at these time intervals (frequency ranges). Beyond the synchronization regions, the phase difference rapidly varies in time; this behavior stems from a complex chaotic dynamics of the CVS in humans, similarly to the case with the Rössler oscillator (cf. with the curves in Fig. 6).

Three regions of different-order synchronization can be set off at different time intervals in Fig. 8. First, the 1 : 1 synchronization is observed in the range 200–500 s (region *A*), where the breathing frequency is close to the frequency of the Mayer wave, 0.1 Hz. Second, the 1 : 2 synchronization is observed at the range 1050 to 1200 s (region *B*), where the breathing frequency approaches the second harmonic of the Mayer wave, 0.2 Hz. Finally, the time range 1380–1520 s (region *C*) also contains a portion of monotonically varying phase difference corresponding to the 2 : 5 synchronization. In this case, the frequency of the external action (breathing) equals 0.25 Hz.

Note that the regions of different-order synchronization are distinctly seen in all the time dependences of the phase difference plotted using different wavelets. This fact supports the conclusion about the presence of synchronization between the breathing rhythm and the rhythm of the slow regulation of arterial pressure.

A number of dependences of the phase difference calculated at different parameters of the generating wavelet show the same features that have been found upon studying the synchronization of the asymmetric van der Pol oscillator by an external action with a variable frequency. In particular, a higher parameter τ results in a larger swing of the phase difference as it varies monotonically within the synchronization range (this is clearly seen from comparison of curves *1* and *2* in Fig. 8 at the 1 : 1 synchronization region (region *A*)). At $\tau = -5.25$ s, the behavior of phase difference qualitatively changes: $\Delta\varphi_0(t)$ decreases with time, thus, making the regions of synchronous dynamics more distinct and easier to identify (see Fig. 8, curve *3*, region *A*).

It can be inferred that, at certain time scales (and, accordingly, certain frequency bands), the respiratory dynamics manifesting itself in the series of the *R–R* intervals produces an effect on the internal rhythm of the Mayer wave in the human CVS. Three synchronization regions of the (1 : 1), (1 : 2), and (2 : 5) orders were detected.

It is worth noting that the proposed method offers a fairly high sensitivity: analysis of a single scalar time series makes it possible to detect three regions with different orders of synchronization. In our earlier study [18], where the wavelet transforms of the series of *R–R* intervals and breathing were calculated along a variable time scale (corresponding to a linearly growing frequency of breathing), we managed to detect only the simplest synchronization type (1 : 1) observed when the breathing frequency coincides with the frequency of the Mayer wave. Compared to the previous results, the method proposed here provides a more accurate and detailed analysis of synchronization between the rhythms of the human CVS and respiratory system.

CONCLUSIONS

A new method is proposed for detecting synchronization of self-sustained oscillations by an external action using univariant data (a single time series characterizing the response of the oscillator on the external action). In essence, the method is based on the time analysis of the instantaneous phase difference resulting from a continuous wavelet transform with the Morlet generating wavelet at the time scale corresponding to the fundamental frequency of the self-sustained oscillations. The necessary condition for applicability of the method is the use of external action with frequency modulation, as proposed in [17, 18]. Tests carried out for a number of models confirmed the efficacy of the method for detecting synchronization using a scalar signal under a high level of noise and inexact tuning to the basic time scale.

It is also shown that the proposed method allows effective discrimination of the case when external action leads to synchronization from the case when the external signal does not lead to synchronization (and, probably, does not even affect the oscillation dynamics) but appears as an admixture to the detected signal. The need for methods providing effective discrimination between the cases of synchronization and admixing in application to physiological data was noted in [5, 18].

The proposed method was applied to study the interaction between the rhythms of the human cardiovascular and respiratory systems under the drive action of breathing with its frequency growing linearly in time. The analyzed series of *R–R* intervals were extracted from the electrocardiograms of the voluntary participants of the experiments. The investigation showed that the breathing rhythm actively influences the dynamics of slow regulation of the blood pressure with a frequency of 0.1 Hz. In particular, three synchronization modes of orders (1 : 1), (1 : 2), and (2 : 5) were revealed. This result seems to be highly significant since it provides an insight into the dynamics of interaction between such important physiological human subsystems as the cardiovascular and respiratory systems and opens a possibility of new diagnostic methods in the cardiovascular area.

ACKNOWLEDGMENTS

This work was supported by the Russian Foundation for Basic Research (project nos. 03-02-17593 and 05-02-16273) and the "Program of the President of the Russian Federation in Support of Leading Scientific Schools" (grant no. NSh-4167.2006.2).

A.E.H. acknowledges the support from CRDF, project no. Y2-P-06-06. M.D.P. acknowledges the financial support from INTAS, grant no. 03-55-920. A.E.H. and A.A.K. are grateful to the "Dynasty" Noncommercial Program Foundation for financial support.

REFERENCES

1. I. I. Blekhman, *Synchronization of Dynamic Systems* (Nauka, Moscow, 1971) [in Russian].
2. I. I. Blekhman, *Synchronization in Science and Technology* (Nauka, Moscow, 1981; ASME, New York, 1988).
3. A. Pikovsky, M. Rosenblum, and J. Kurths, *Synchronization: Universal Concept in Nonlinear Sciences* (Cambridge Univ. Press, Cambridge, 2001; Tekhnosfera, Moscow, 2003).
4. S. Boccaletti, J. Kurths, G. Osipov, et al., Phys. Rep. **366**, 1 (2002).
5. F. C. Meinecke, A. Ziehe, J. Kurths, and K.-R. Müller, Phys. Rev. Lett. **94**, 084102 (2005).
6. A. E. Hramov and A. A. Koronovskii, Chaos **14**, 603 (2004).
7. A. E. Hramov, A. A. Koronovskii, M. K. Kurovskaya, and O. J. Moskalenko, Phys. Rev. E **71**, 056204 (2005).
8. L. M. Pecora and T. L. Carroll, Phys. Rev. Lett. **64**, 821 (1990).
9. L. M. Pecora, T. L. Carroll, G. A. Jonson, and D. J. Mar, Chaos **7**, 520 (1997).
10. A. Pikovsky, M. Rosenblum, and J. Kurths, Int. J. Bifurcation Chaos Appl. Sci. Eng. **10**, 2291 (2000).
11. S. Boccaletti, L. M. Pecora, and A. Pelaez, Phys. Rev. E **63**, 066219 (2001).
12. N. F. Rulkov, M. M. Sushchik, L. S. Tsimring, and H. D. I. Abarbanel, Phys. Rev. E **51**, 980 (1995).
13. K. Pyragas, Phys. Rev. E **54**, R4508 (1996).
14. P. A. Tass, et al., Phys. Rev. Lett. **81**, 3291 (1998).
15. P. A. Tass, et al., Phys. Rev. Lett. **90**, 088101 (2003).
16. V. S. Anishchenko, A. G. Balanov, N. B. Janson, et al., Int. J. Bifurcation Chaos Appl. Sci. Eng. **10**, 2339 (2000).
17. M. D. Prokhorov, V. I. Ponomarenko, V. I. Gridnev, et al., Phys. Rev. E **68**, 041913 (2003).
18. A. E. Hramov, A. A. Koronovskii, V. I. Ponomarenko, and M. D. Prokhorov, Phys. Rev. E **73**, 026208 (2006).
19. M. Chavez, C. Adam, V. Navarro, et al., Chaos **15**, 023904 (2005).
20. A. E. Hramov, A. A. Koronovskiĭ, and Yu. I. Levin, Zh. Éksp. Teor. Fiz. **127**, 886 (2005) [JETP **100**, 784 (2005)].
21. A. E. Hramov and A. A. Koronovskii, J. Phys. D **206**, 252 (2005).
22. S. Malpas, Am. J. Physiol. Heart Circ. Physiol. **282**, H6 (2002).
23. A. Stefanovska and M. Hočič, Prog. Theor. Phys. Supp. **139**, 270 (2000).
24. C. Schäfer, M. G. Rosenblum, H.-H. Abel, and J. Kurths, Phys. Rev. E **60**, 857 (1999).
25. M. Bračič-Lotrič and A. Stefanovska, J. Phys. A **283**, 451 (2000).
26. S. Rzeczinski, N. B. Janson, A. G. Balanov, and P. V. E. McClintock, Phys. Rev. E **66**, 051909 (2002).
27. A. E. Hramov, A. A. Koronovskii, V. I. Ponomarenko, and M. D. Prokhorov, in *Proceedings of the International Symposium on Topical Problems of Nonlinear Wave Physics, N. Novgorod, 2005*, Part 1, p. 33.
28. A. A. Koronovskii, V. I. Ponomarenko, M. D. Prokhorov, and A. E. Hramov, Radiotekh. Élektron. (Moscow) **52**, (2007) (in Press).
29. N. B. Janson, A. G. Balanov, V. S. Anishchenko, and P. V. E. McClintock, Phys. Rev. E **65**, 036211 (2002).
30. A. G. Rossberg, K. Bartholomo, H. U. Voss, and J. Timmer, Phys. Rev. Lett. **93**, 154103 (2004).
31. N. B. Janson, A. G. Balanov, V. S. Anishchenko, and P. V. E. McClintock, Phys. Rev. E **65**, 036212 (2002).
32. V. I. Ponomarenko, M.D. Prokhorov, A. B. Bespyatov, et al., Chaos, Solitons, Fractals **23**, 1429 (2005).
33. O. E. Rössler, Phys. Lett. A **57**, 397 (1976).
34. A. A. Koronovskii and A. E. Hramov, Pis'ma Zh. Éksp. Teor. Fiz. **79**, 391 (2004) [JETP Lett. **79**, 316 (2004)].
35. *Wavelets in Physics*, Ed. by J. C. Van den Berg (Cambridge Univ., Cambridge, 2004).
36. A. A. Koronovskii and A. E. Hramov, *Continuous Wavelet Analysis and Its Applications* (Fizmatlit, Moscow, 2003) [in Russian].
37. A. Grossman and J. Morlet, SIAM J. Matrix Anal. Appl. **15**, 273 (1984).
38. R. Adler, Proc. IRE **34**, 351 (1949).
39. W. H. Press, S. A. Teukolsky, W. T. Vetterling, and B. T. Flannery, *Numerical Recipes* (Cambridge Univ., Cambridge, 1997).
40. J. B. Bassingthwaighte, L. S. Liebovitch, and B. J. West, *Fractal Physiology* (Oxford Univ., New York, 1994).

Translated by A. Sidorova